J. Plasma Phys. (2019), *vol.* 85, 775850501
doi:10.1017/S0022377819000576

Magnetic helicity in multiply connected domains

D. MacTaggart[1,2,†] **and A. Valli**[1]

[1]Department of Mathematics, University of Trento, Povo, Italy

[2]School of Mathematics and Statistics, University of Glasgow, Glasgow G12 8QW, UK

(Received 6 June 2019; revised 10 August 2019; accepted 12 August 2019)

Magnetic helicity is a fundamental quantity of magnetohydrodynamics that carries topological information about the magnetic field. By 'topological information', we usually refer to the linkage of magnetic field lines. For domains that are not simply connected, however, helicity also depends on the topology of the domain. In this paper we expand the standard definition of magnetic helicity in simply connected domains to multiply connected domains in $\mathbb{R}^3$ of arbitrary topology. We also discuss how using the classic Biot–Savart operator simplifies the expression for helicity and how domain topology affects the physical interpretation of helicity.

Key words: plasma properties, plasma nonlinear phenomena

1. Introduction

The classical definition of magnetic helicity in magnetohydrodynamics (MHD) is for a bounded simply connected domain. Let Ω be such a domain with boundary $\partial\Omega$ and outward unit normal $\boldsymbol{n}$. Consider a magnetic field $\boldsymbol{B}$ in the space

$$\mathcal{V} = \{\boldsymbol{B} \in (L^2(\Omega))^3 : \operatorname{div}\boldsymbol{B} = 0, \boldsymbol{B}\cdot\boldsymbol{n} = 0\}. \tag{1.1}$$

Then the magnetic helicity (hereafter helicity) is

$$H = \int_\Omega \boldsymbol{A}\cdot\boldsymbol{B}, \tag{1.2}$$

where $\boldsymbol{B} = \operatorname{curl}\boldsymbol{A}$. It is well known that H is an invariant of ideal MHD (Woltjer 1958) and is also well conserved in resistive MHD with very small magnetic diffusion (Berger 1984; Faraco & Lindberg 2018). It is also well known that H is gauge invariant, that is, H is not affected by the change $\boldsymbol{A} \to \boldsymbol{A} + \operatorname{grad}\chi$, for some scalar function χ.

The topological interpretation of H is due, originally, to Moffatt (1969). By considering the Coulomb gauge, $\operatorname{div}\boldsymbol{A} = 0$, Moffatt (1969) showed that H could be interpreted in terms of the Gauss linking number weighted by magnetic flux. The linking number can refer to the linkage of thin flux tubes (e.g. Moffatt 1969) or field lines (e.g. Arnold & Khesin 1992). Since both helicity and magnetic flux are

† Email address for correspondence: david.mactaggart@glasgow.ac.uk

invariants of ideal MHD, this linkage is also invariant. The topology of field lines has also been studied in magnetic fields that are not everywhere tangent to the domain boundary (e.g. Berger & Field 1984) but we will not consider such fields in this work.

Moving to multiply connected domains, there have been two general approaches to determining helicity. The first comes from plasma physics and focuses on a toroidal domain suitable for fusion devices (e.g. Taylor & Newton 2015). This domain is not simply connected and H from (1.2) is not (in general) gauge invariant in such a domain. The main reference in the plasma physics literature to the gauge-invariant form of helicity in a torus is Bevir & Gray (1980), who state that the correct form of helicity is

$$H = \int_{\Omega} \boldsymbol{A} \cdot \boldsymbol{B} - \oint_{\gamma_1} \boldsymbol{A} \cdot \boldsymbol{t}_1 \oint_{\gamma_2} \boldsymbol{A} \cdot \boldsymbol{t}_2, \tag{1.3}$$

where Ω no longer refers to a simply connected domain (which will be assumed for the rest of this work), γ_1 and γ_2 are closed paths on $\partial\Omega$ travelling around the major and minor circumferences of the torus, respectively, and $\boldsymbol{t}_1$ and $\boldsymbol{t}_2$ are the associated unit tangent vectors of the paths. The derivation of (1.3), which we refer to as the Bevir–Gray formula, in the plasma physics literature is based on making the transformation $\boldsymbol{A} \to \boldsymbol{A} + \operatorname{grad}\chi$ but with χ now being multivalued (e.g. Biskamp 1993; Marsh 1996). After the transformation is performed, the domain is cut in order to make χ single-valued, and the result is the second term on the right-hand side of (1.3). This approach is difficult to generalize to domains of more complex topology. Later, we will derive a generalized version of the Bevir–Gray formula by means of the Helmholtz decomposition of vectors in multiply connected domains.

Whereas the approach in plasma physics has been to focus on a particular domain and not specify a particular vector potential, the second approach to determining helicity in multiply connected domains has been to specify the vector potential and consider arbitrary domains. In a series of papers by Cantarella and collaborators (Cantarella 2000; Cantarella *et al.* 2000; Cantarella, DeTurck & Gluck 2001, 2002), the vector potential is chosen to satisfy the Coulomb gauge and takes the form of the Biot–Savart operator,

$$\mathrm{BS}(\boldsymbol{B})(\boldsymbol{x}) = \frac{1}{4\pi} \int_{\Omega} \boldsymbol{B}(\boldsymbol{y}) \times \frac{\boldsymbol{x}-\boldsymbol{y}}{|\boldsymbol{x}-\boldsymbol{y}|^3}\, \mathrm{d}\boldsymbol{y}. \tag{1.4}$$

This operator appears in other contexts in electromagnetism and, as mentioned previously, was used in Moffatt (1969) to interpret helicity in terms of the Gauss linking number.[1] One particularly interesting property of the Biot–Savart operator is that it can be made self-adjoint, leading to the application of spectral theory where magnetic fields that maximize the helicity in a domain correspond to linear force-free fields (e.g. Cantarella *et al.* 2000; Valli 2019). In this paper, we will refer to helicity expressed in terms of the Biot–Savart operator as Biot–Savart helicity. This term is purely for convenience and does not imply a new object: Biot–Savart helicity is still helicity but written in a particular way.

In this work we show that the two approaches to finding helicity in multiply connected domains, described above, can be unified. We first generalize (1.3) to

[1] When Gauss's formula was published officially in 1867, it was included as part of a collection of material relating to electromagnetic induction (Epple 1998). This represents one of the many early links between topology and electromagnetism.

https://doi.org/10.1017/S0022377819000576 Published online by Cambridge University Press

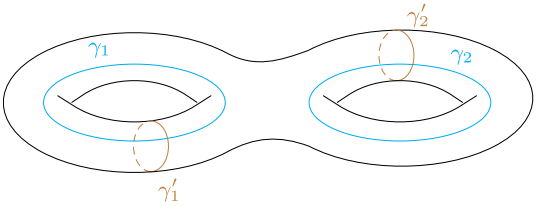

FIGURE 1. A domain with $g=2$. The cycles are shown in brown and cyan, following the notation in the main text. The oriented surfaces bounded by the cycles γ_j' and γ_j define the cutting surfaces Σ_j and Σ_j', respectively.

connected domains of arbitrary topology in a systematic way. We then show how the gauge-invariant helicity in multiply connected domains is coincident with Biot–Savart helicity. This leads to a discussion of how the (often quoted) mutual helicity (Moffatt 1969; Laurence & Avellaneda 1993; Cantarella 2000) follows from the general helicity formula. The paper ends with a summary and a discussion of the interpretation of helicity in periodic domains.

2. Helicity in multiply connected domains

2.1. *Geometrical set-up*

We now describe the general geometrical set-up and introduce ideas from homology which are necessary for treating multiply connected domains. A comprehensive review of the application of homology to magnetic fields can be found in Blank, Friedrichs & Grad (1957). A more recent and accessible account can be found in Cantarella *et al.* (2002).

We consider a domain $\Omega \in \mathbb{R}^3$ that is a bounded open connected set with Lipschitz continuous boundary $\partial\Omega$ and outer unit normal vector $\boldsymbol{n}$. If the first Betti number of Ω is (the genus) $g>0$, then the first Betti number of $\partial\Omega$ is $2g$ (e.g. Cantarella *et al.* 2002). We can consider $2g$ non-bounding cycles on $\partial\Omega$, $\{\gamma_j\}_{j=1}^g \cup \{\gamma_j'\}_{j=1}^g$, that represent the generators of the first homology group of $\partial\Omega$. Each set of cycles is associated with the closed domain and its complement in a ball containing the domain. The $\{\gamma_j\}_{j=1}^g$ represent the generators of the first homology group of $\overline{\Omega}$ and have unit tangent vectors denoted by $\boldsymbol{t}_j$. The $\{\gamma_j'\}_{j=1}^g$ represent the generators of the first homology group of $\overline{\Omega'}$, where $\Omega' = B \setminus \overline{\Omega}$ and B is an open ball containing $\overline{\Omega}$. The unit tangent vector of a cycle γ_j' is denoted $\boldsymbol{t}_j'$.

In Ω there are g cutting surfaces, $\{\Sigma\}_{j=1}^g$, that are connected orientable Lipschitz surfaces satisfying $\Sigma_j \subset \Omega$ and $\partial\Sigma_j \subset \partial\Omega$. Each surface Σ_j satisfies $\partial\Sigma_j = \gamma_j'$ and cuts the cycle γ_j. A similar set of cutting surfaces, $\{\Sigma'\}_{j=1}^g$, exists in Ω'. An illustration of the geometrical set-up for a domain with $g=2$ is shown in figure 1. For the sake of definiteness, we choose the unit normal vector $\boldsymbol{n}_{\Sigma_j}$ on Σ_j oriented in such a way that (i) the unit tangent vector $\boldsymbol{t}_j'$ on $\gamma_j' = \partial\Sigma_j$ is oriented counterclockwise with respect to $\boldsymbol{n}_{\Sigma_j}$ (the 'right-hand rule') and (ii) the unit tangent vector $\boldsymbol{t}_j$ crosses Σ_j consistently with the direction of $\boldsymbol{n}_{\Sigma_j}$.

In the above description, if the boundary of Ω is not connected then some care needs to be taken to make sure that a particular cutting surface remains in Ω or Ω' but not in both. For the n-holed torus, such as the two-holed torus in figure 1, this is not an issue. For a toroidal shell (e.g. O'Neil & Cerfon 2018), however, the

https://doi.org/10.1017/S0022377819000576 Published online by Cambridge University Press

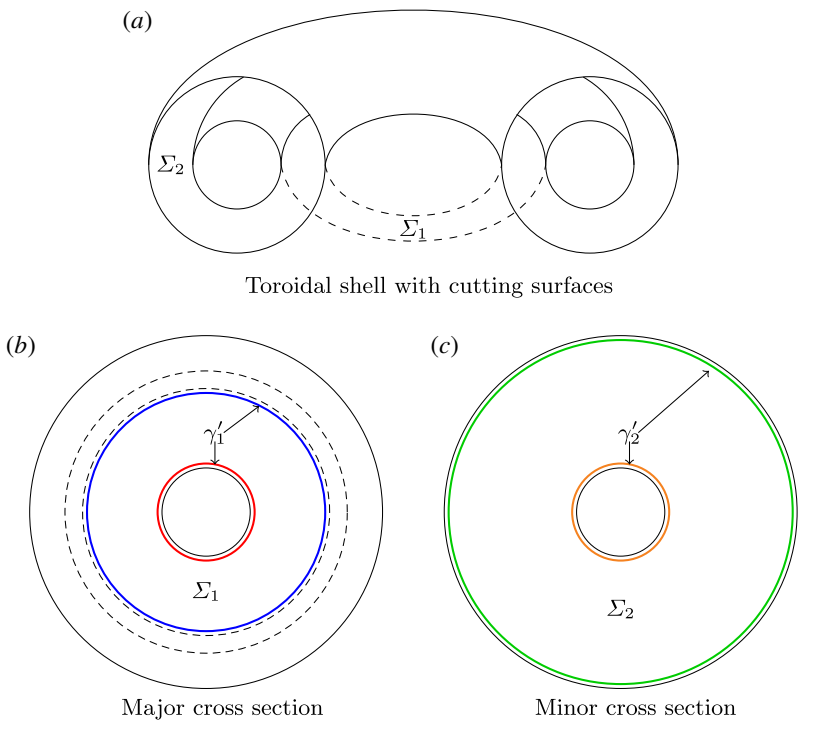

FIGURE 2. Toroidal shell with cutting surfaces. (*a*) A three-dimensional illustration of a toroidal shell cut in half. The cutting surfaces Σ_1 and Σ_2 are indicated. (*b*) The major cross-section (toroidal hole shown as dashed lines) where γ_1' is the boundary of the annulus Σ_1 represented by the blue and red cycles. (*c*) The minor cross-section where γ_2' is the boundary of the annulus Σ_2 represented by the orange and green cycles. Note that the cross-sections are not to scale.

boundary is not connected, that is, the outer boundary of the solid torus is separated from the inner boundary of the toroidal hole. A toroidal shell has $g=2$ and so there are two cycles for Ω and two for Ω'. It is easy to see that the cutting surfaces Σ_j', corresponding to the γ_j, lie entirely in Ω'. Naively performing the same procedure for the cutting surfaces Σ_j of the γ_j', however, results in their overlapping with parts of the complementary domain Ω'. Restricting the Σ_j to lie entirely in Ω can be achieved using homological properties. We explain the procedure by describing the cutting surfaces for the cycles, γ_1' and γ_2', which orbit the central hole of the torus and the toroidal hole, respectively. This situation is illustrated in figure 2.

The boundary of the first cutting surface, $\partial\Sigma_1=\gamma_1'$, is indicated in figure 2(*b*) by the red and blue cycles. Similarly, the boundary of the other cutting surface, $\partial\Sigma_2=\gamma_2'$, is indicated in figure 2(*c*) by orange and green cycles. The surfaces Σ_1 and Σ_2 lie entirely in Ω and are annuli.

For a given orientation of the normal $\boldsymbol{n}_1$ of Σ_1,

$$\int_{\Sigma_1}\mathrm{curl}\boldsymbol{w}\cdot\boldsymbol{n}_1=\int_{\text{blue}}\boldsymbol{w}\cdot\boldsymbol{t}_1'-\int_{\text{red}}\boldsymbol{w}\cdot\boldsymbol{t}_1', \tag{2.1}$$

where $\boldsymbol{w}$ is a vector field and 'blue' and 'red' represent the cycles displayed in figure 2(*b*). A similar result holds for Σ_2. Note, however, that the red cycle is

https://doi.org/10.1017/S0022377819000576 Published online by Cambridge University Press

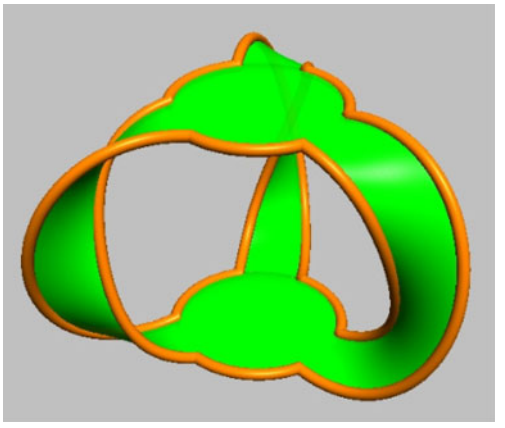

FIGURE 3. An example of a 'cut' domain that is not simply connected. Following the description in the main text, the orange domain is the trefoil knot K. The green surface is one of the cutting surfaces, shown here as two 'discs' with three 'twisting bands'. This image was produced with SeifertView (Jarke J. van Wijk, Technische Universiteit Eindhoven).

bounding in Ω', thus γ_1' and the blue cycle are equivalent homologically. The same is true for γ_2' and the green cycle in figure 2(*c*).

In this paper we will focus on (n-holed) tori and toroidal shells since these domains have the most immediate applications, both as domains in their own right (e.g. Dewar *et al.* 2015; O'Neil & Cerfon 2018) and in their connection to the common simulation domains of periodic and doubly periodic cubes (we will return to discuss helicity in periodic domains later). The 'cut' domains (those formed by removing the cutting surfaces) for these cases are simply connected. This fact, however, is not true of all domains in $\mathbb{R}^3$. For example, consider a domain $\Omega = B \setminus K$ where B is a ball, as before, and K is a trefoil knot (Benedetti, Frigerio & Ghiloni 2012; Alonso Rodríguez *et al.* 2018). An illustration of such a domain is displayed in figure 3. The procedure that we will now describe can cope with all the cases described above, including this last one.

2.2. *Helmholtz decomposition and Neumann harmonic vector fields*

The gauge transformation normally used in helicity studies, $\boldsymbol{A} \to \boldsymbol{A} + \operatorname{grad}\chi$, is only applicable in simply connected domains if χ is to remain single-valued. For the regions under consideration with more complex topologies, we require the full Helmholtz decomposition (e.g. Blank *et al.* 1957; Cantarella *et al.* 2002).

THEOREM 1 (Helmholtz). *Any* $\boldsymbol{u} \in (L^2(\Omega))^3$ *can be decomposed as*

$$\boldsymbol{u} = \operatorname{curl}\boldsymbol{P} + \operatorname{grad}\phi + \boldsymbol{\rho}, \tag{2.2}$$

where $\boldsymbol{P}$ *is a vector field,* ϕ *a single-valued scalar function and* $\boldsymbol{\rho}$ *is in the space of Neumann harmonic fields* $\mathcal{H}$*, defined as*

$$\mathcal{H} = \{\boldsymbol{\rho} \in (L^2(\Omega))^3 : \operatorname{curl}\boldsymbol{\rho} = \boldsymbol{0},\ \operatorname{div}\boldsymbol{\rho} = 0,\ \boldsymbol{\rho}\cdot\boldsymbol{n} = 0\}. \tag{2.3}$$

https://doi.org/10.1017/S0022377819000576 Published online by Cambridge University Press

In order to make use of $\mathcal{H}$, we need its basis $\{\boldsymbol{\rho}_j\}_{j=1}^g$. This can be found, for both Ω and Ω' separately, by finding the solutions ϕ_j of suitable elliptic problems where the appropriate cutting surfaces are removed from the domain under study. The basis functions for the space of harmonic fields in Ω take the form $\boldsymbol{\rho}_j = \widetilde{\operatorname{grad}}\,\phi_j$, where $\widetilde{\operatorname{grad}}\,\phi_j$ is the extension of $\operatorname{grad}\phi_j$ to $(L^2(\Omega))^3$ and each ϕ_j has a jump equal to 1 on the corresponding cutting surface. The basis functions of the space of harmonic fields in Ω' are constructed in a similar way and are denoted by $\{\boldsymbol{\rho}_j'\}_{j=1}^g$. For more details on the construction of the basis functions, we direct the reader to Alonso Rodríguez *et al.* (2018).

2.3. *Zero flux magnetic fields*

Consider two different vector potentials $\boldsymbol{A}_1$ and $\boldsymbol{A}_2$ for $\boldsymbol{B} \in \mathcal{V}$. Since $\operatorname{curl}(\boldsymbol{A}_1 - \boldsymbol{A}_2) = \boldsymbol{0}$ in Ω, it follows from Theorem 1 that we can write

$$\boldsymbol{A}_1 - \boldsymbol{A}_2 = \operatorname{grad}\chi + \boldsymbol{\rho} \ \text{ in } \ \Omega, \tag{2.4}$$

where χ is a scalar function and $\boldsymbol{\rho} \in \mathcal{H}$. Some simple manipulation reveals

$$\int_\Omega \boldsymbol{A}_1 \cdot \boldsymbol{B} - \int_\Omega \boldsymbol{A}_2 \cdot \boldsymbol{B} = \int_\Omega \boldsymbol{B} \cdot \boldsymbol{\rho}. \tag{2.5}$$

Therefore, if $\boldsymbol{B} \perp \mathcal{H}$ then helicity is independent of the vector potential. Writing $\boldsymbol{\rho}$ in terms of its basis functions, we require that

$$\int_\Omega \boldsymbol{B} \cdot \boldsymbol{\rho}_j = 0, \quad \text{for } j = 1, \ldots, g. \tag{2.6}$$

This statement is nothing more than enforcing zero magnetic flux through every cutting surface,

$$\begin{aligned} \int_\Omega \boldsymbol{B} \cdot \boldsymbol{\rho}_j \ &= \int_{\Omega \setminus \Sigma_j} \boldsymbol{B} \cdot \boldsymbol{\rho}_j = \int_{\Omega \setminus \Sigma_j} \boldsymbol{B} \cdot \operatorname{grad}\phi_j \\ &= \int_{\partial(\Omega \setminus \Sigma_j)} \boldsymbol{B} \cdot \boldsymbol{n}_j \phi_j - \int_{\Omega \setminus \Sigma_j} (\operatorname{div}\boldsymbol{B})\phi_j \\ &= \int_{\Sigma_j} \boldsymbol{B} \cdot \boldsymbol{n}_j [[\phi_j]] = \int_{\Sigma_j} \boldsymbol{B} \cdot \boldsymbol{n}_j, \end{aligned} \tag{2.7}$$

where $[[\phi_j]] = \phi_j|_{\Sigma_j^+} - \phi_j|_{\Sigma_j^-} = 1$, from the construction of the basis functions (Alonso Rodríguez *et al.* 2018). Thus, by enforcing zero magnetic flux through all the cutting surfaces of Ω, the helicity in the domain can be written as in (1.2).

This approach to defining helicity in multiply connected domains has been used in several theoretical works (e.g. Jordan, Yoshida & Ito 1998; Faraco & Lindberg 2018). For cases where there is non-zero magnetic flux, more work is needed to produce a gauge-invariant helicity. We will now derive a more general formula which includes the zero flux condition as a special case.

2.4. *Generalized Bevir–Gray formula*

Let us consider the following quantities,

$$H_1 = \int_\Omega \boldsymbol{A}_1 \cdot \boldsymbol{B}, \quad H_2 = \int_\Omega \boldsymbol{A}_2 \cdot \boldsymbol{B}, \tag{2.8a,b}$$

https://doi.org/10.1017/S0022377819000576 Published online by Cambridge University Press

where $\boldsymbol{B} = \operatorname{curl}\boldsymbol{A}_1$ and $\boldsymbol{B} = \operatorname{curl}\boldsymbol{A}_2$, respectively. Without the zero flux condition, H_1 and H_2 are not, in general, gauge invariant in multiply connected domains. Considering the difference of these quantities,

$$\begin{aligned} H_1 - H_2 &= \int_\Omega \boldsymbol{B}\cdot(\boldsymbol{A}_1 - \boldsymbol{A}_2) = \int_\Omega \operatorname{curl}\boldsymbol{A}_1\cdot(\boldsymbol{A}_1 - \boldsymbol{A}_2) \\ &= \int_{\partial\Omega} \boldsymbol{n}\times\boldsymbol{A}_1\cdot(\boldsymbol{A}_1 - \boldsymbol{A}_2) = \int_{\partial\Omega} \boldsymbol{A}_1\times\boldsymbol{n}\cdot\boldsymbol{A}_2. \end{aligned} \tag{2.9}$$

The second line follows from integration by parts and using $\operatorname{curl}(\boldsymbol{A}_1 - \boldsymbol{A}_2) = \boldsymbol{0}$. Since $\operatorname{curl}\boldsymbol{A}_1\cdot\boldsymbol{n} = 0 = \operatorname{curl}\boldsymbol{A}_2\cdot\boldsymbol{n}$, the tangential traces $\boldsymbol{A}_1\times\boldsymbol{n}$ and $\boldsymbol{A}_2\times\boldsymbol{n}$ can be expressed, via a Helmholtz decomposition on $\partial\Omega$ (e.g. Hiptmair, Kotiuga & Tordeux 2012; Alonso Rodríguez *et al.* 2018), as

$$\boldsymbol{A}_1\times\boldsymbol{n} = \operatorname{grad}\eta\times\boldsymbol{n} + \sum_{j=1}^{g}\alpha_j\boldsymbol{\rho}_j\times\boldsymbol{n} + \sum_{j=1}^{g}\beta_j\boldsymbol{\rho}_j'\times\boldsymbol{n}, \tag{2.10}$$

$$\boldsymbol{A}_2\times\boldsymbol{n} = \operatorname{grad}\xi\times\boldsymbol{n} + \sum_{j=1}^{g}\delta_j\boldsymbol{\rho}_j\times\boldsymbol{n} + \sum_{j=1}^{g}\mu_j\boldsymbol{\rho}_j'\times\boldsymbol{n}, \tag{2.11}$$

where η, ξ are scalar functions and $\alpha_j, \beta_j, \delta_j, \mu_j \in \mathbb{R}$ $(j = 1, \ldots, g)$. Alonso Rodríguez *et al.* (2018) derived the following useful identities:

$$\left.\begin{gathered} \int_{\partial\Omega}\operatorname{grad}\eta\times\boldsymbol{n}\cdot\operatorname{grad}\xi = 0, \\ \int_{\partial\Omega}\operatorname{grad}\eta\times\boldsymbol{n}\cdot\boldsymbol{\rho}_j = 0, \quad \int_{\partial\Omega}\operatorname{grad}\eta\times\boldsymbol{n}\cdot\boldsymbol{\rho}_i' = 0, \\ \int_{\partial\Omega}\boldsymbol{\rho}_i\times\boldsymbol{n}\cdot\boldsymbol{\rho}_j = 0, \quad \int_{\partial\Omega}\boldsymbol{\rho}_i'\times\boldsymbol{n}\cdot\boldsymbol{\rho}_j' = 0, \\ \int_{\partial\Omega}\boldsymbol{\rho}_j\times\boldsymbol{n}\cdot\boldsymbol{\rho}_i' = \delta_{ij} = -\int_{\partial\Omega}\boldsymbol{\rho}_i'\times\boldsymbol{n}\cdot\boldsymbol{\rho}_j, \end{gathered}\right\} \tag{2.12}$$

for $1 \leqslant i, j \leqslant g$. Note that δ_{ij} is the Kronecker delta. By making use of (2.10) and (2.11) and the above identities, it can be shown that

$$\int_{\partial\Omega}\boldsymbol{A}_1\times\boldsymbol{n}\cdot\boldsymbol{A}_2 = \sum_{j=1}^{g}\alpha_j\mu_j - \sum_{j=1}^{g}\beta_j\delta_j, \tag{2.13}$$

where

$$\alpha_j = \oint_{\gamma_j}\boldsymbol{A}_1\cdot\boldsymbol{t}_j, \quad \beta_j = \oint_{\gamma_j'}\boldsymbol{A}_1\cdot\boldsymbol{t}_j', \tag{2.14a,b}$$

$$\delta_j = \oint_{\gamma_j}\boldsymbol{A}_2\cdot\boldsymbol{t}_j, \quad \mu_j = \oint_{\gamma_j'}\boldsymbol{A}_2\cdot\boldsymbol{t}_j'. \tag{2.15a,b}$$

Since $\gamma_j' = \partial\Sigma_j$, we have, by Stokes's theorem,

$$\beta_j = \oint_{\gamma_j'}\boldsymbol{A}_1\cdot\boldsymbol{t}_j' = \int_{\Sigma_j}\operatorname{curl}\boldsymbol{A}_1\cdot\boldsymbol{n}_j = \int_{\Sigma_j}\boldsymbol{B}\cdot\boldsymbol{n}_j. \tag{2.16}$$

https://doi.org/10.1017/S0022377819000576 Published online by Cambridge University Press

By exactly the same reasoning,

$$\mu_j = \oint_{\gamma_j'} \boldsymbol{A}_2 \cdot \boldsymbol{t}_j' = \int_{\Sigma_j} \boldsymbol{B} \cdot \boldsymbol{n}_j. \tag{2.17}$$

Putting all these results together, we can now write

$$H_1 - H_2 = \int_\Omega \boldsymbol{A}_1 \cdot \boldsymbol{B} - \int_\Omega \boldsymbol{A}_2 \cdot \boldsymbol{B} = \sum_{j=1}^{g} \left(\oint_{\gamma_j} \boldsymbol{A}_1 \cdot \boldsymbol{t}_j - \oint_{\gamma_j} \boldsymbol{A}_2 \cdot \boldsymbol{t}_j \right) \left(\int_{\Sigma_j} \boldsymbol{B} \cdot \boldsymbol{n}_j \right). \tag{2.18}$$

An alternative route to (2.18) is to consider a result from Blank *et al.* (1957). Based on the consideration of vector identities, they derive a particular formula (see their formula (6.5) on page 65) for the inner product of an irrotational vector $\boldsymbol{x}$ and a solenoidal vector $\boldsymbol{y}$,

$$\int_\Omega \boldsymbol{x} \cdot \boldsymbol{y} = \sum_{j=1}^{g} \oint_{\gamma_j} \boldsymbol{x} \cdot \boldsymbol{t}_j \int_{\Sigma_j} \boldsymbol{y} \cdot \boldsymbol{n}_j, \tag{2.19}$$

where the notation for cycles and surfaces is as before and the vector fields are everywhere tangent to the boundary. In our application, $\boldsymbol{x} = \boldsymbol{A}_1 - \boldsymbol{A}_2$ and $\boldsymbol{y} = \boldsymbol{B}$.

Returning to (2.18), it is clear that the quantity

$$\int_\Omega \boldsymbol{A} \cdot \boldsymbol{B} - \sum_{j=1}^{g} \left(\oint_{\gamma_j} \boldsymbol{A} \cdot \boldsymbol{t}_j \right) \left(\int_{\Sigma_j} \boldsymbol{B} \cdot \boldsymbol{n}_j \right) \tag{2.20}$$

is independent of the choice of vector potential. We are, therefore, led to define the gauge-invariant magnetic helicity as

$$\Upsilon(\boldsymbol{B}) = \int_\Omega \boldsymbol{A} \cdot \boldsymbol{B} - \sum_{j=1}^{g} \left(\oint_{\gamma_j} \boldsymbol{A} \cdot \boldsymbol{t}_j \right) \left(\int_{\Sigma_j} \boldsymbol{B} \cdot \boldsymbol{n}_j \right). \tag{2.21}$$

It is clear that for $g = 1$, equation (2.21) reduces to the Bevir–Gray formula. Also, if $\boldsymbol{B} \perp \mathcal{H}$ (zero flux), the helicity reduces to

$$\Upsilon(\boldsymbol{B}) = \int_\Omega \boldsymbol{A} \cdot \boldsymbol{B}. \tag{2.22}$$

This is also the case for simply connected domains, for which $\mathcal{H} = \{\boldsymbol{0}\}$.

2.5. *Biot–Savart helicity*

As mentioned before, apart from the application of the Bevir–Gray formula in toroidal domains, helicity in multiply connected domains has, generally, taken the form of Biot–Savart helicity,

$$H(\boldsymbol{B}) = \int_\Omega \mathrm{BS}(\boldsymbol{B}) \cdot \boldsymbol{B}. \tag{2.23}$$

The Biot–Savart helicity formula resembles that of helicity in simply connected domains, that is to say, the second term on the right-hand side of (2.21) is missing. We will now show that (2.21) and (2.23) are coincident. Following Cantarella *et al.* (2001) and Valli (2019), it can be shown that the Biot–Savart operator, defined on Ω, can be extended to $\mathbb{R}^3$.

https://doi.org/10.1017/S0022377819000576 Published online by Cambridge University Press

For $\boldsymbol{B} \in \mathcal{V}$, $\mathrm{BS}(\boldsymbol{B}) \in \mathcal{V}$. Since $\boldsymbol{B} \cdot \boldsymbol{n} = 0$ on $\partial\Omega$ and $\operatorname{div} \boldsymbol{B} = 0$ in Ω, the extended magnetic field

$$\widetilde{\boldsymbol{B}} = \begin{cases} \boldsymbol{B} & \text{in } \Omega, \\ \boldsymbol{0} & \text{in } \mathbb{R}^3 \setminus \overline{\Omega}, \end{cases} \tag{2.24}$$

satisfies $\operatorname{div} \widetilde{\boldsymbol{B}} = 0$ in $\mathbb{R}^3$.

Equation (1.4) can be modified to

$$\mathrm{BS}(\boldsymbol{B})(\boldsymbol{x}) = \frac{1}{4\pi} \int_{\mathbb{R}^3} \widetilde{\boldsymbol{B}}(\boldsymbol{y}) \times \frac{\boldsymbol{x} - \boldsymbol{y}}{|\boldsymbol{x} - \boldsymbol{y}|^3} \, \mathrm{d}\boldsymbol{y}. \tag{2.25}$$

We know from Cantarella *et al.* (2001) that $\operatorname{curl} \mathrm{BS}(\boldsymbol{B}) = \widetilde{\boldsymbol{B}}$ and $\operatorname{div} \boldsymbol{B} = 0$ in $\mathbb{R}^3$. Therefore, we can consider line integrals along closed paths and apply Stokes's theorem.

2.5.1. *n-holed tori*

We know that each $\Sigma_j' \subset \Omega'$ $(j = 1, \ldots, g)$ is a surface bounded by a simple cycle γ_j (one with a connected boundary). We then have

$$\oint_{\gamma_j} \mathrm{BS}(\boldsymbol{B}) \cdot \boldsymbol{t}_j = \int_{\Sigma_j'} \operatorname{curl} \mathrm{BS}(\boldsymbol{B}) \cdot \boldsymbol{n}_j' = 0, \tag{2.26}$$

since $\operatorname{curl} \mathrm{BS}(\boldsymbol{B}) = \boldsymbol{0}$ in Ω'. Thus, choosing $\boldsymbol{A} = \mathrm{BS}(\boldsymbol{B})$ in (2.21), the helicity reduces to

$$\Upsilon(\boldsymbol{B}) = \int_{\Omega} \mathrm{BS}(\boldsymbol{B}) \cdot \boldsymbol{B}. \tag{2.27}$$

Note that (2.27) can also be used for magnetic fields with zero flux, without having to impose this as a condition to ensure gauge invariance.

In above approach to deriving (2.27) we have made the standard construction of extending the Biot–Savart operator to $\mathbb{R}^3$ by assuming that the magnetic field is zero outside the domain. By virtue of (2.27), the magnetic field in the domain can inherit the field line topology interpretation of Moffatt (1969) and Arnold & Khesin (1992). For applications where linkage with magnetic field outside the domain is important, see § 2.6 below. First, however, we will investigate how the Biot–Savart operator can be used to understand the linkage of field lines on the surface of the domain with the domain itself.

2.5.2. *Field line helicity on a toroidal boundary*

Although the second term on the right-hand side of (2.21), related to the domain topology, is zero for Biot–Savart helicity, this does not mean that integrals on the domain boundary are unimportant. For the case of a standard torus ($g = 1$), the property in (2.26) can be extended to define the field line helicity (e.g. Berger 1988; Yeates & Hornig 2013) on the boundary when the path of integration follows a closed field line. Such field lines are possible everywhere on the boundary of a torus as the Euler characteristic of the boundary is zero. A prominent example of such a field line is a torus knot (e.g. Oberti & Ricca 2018). For domains with $g > 1$, closed field lines on the boundary are possible, but not everywhere on the boundary. This is due

https://doi.org/10.1017/S0022377819000576 Published online by Cambridge University Press

to the Euler characteristic being non-zero and, as a consequence of the 'hairy ball' theorem (e.g. Frankel 2004), smooth vector fields on the surfaces of these domains must have at least one point where they vanish.

A closed path γ on the surface of a torus Ω can be expressed in terms of the basis cycles γ_1 and γ_1' as

$$\gamma = L'\gamma_1 + L\gamma_1', \tag{2.28}$$

up to bounding cycles on $\partial\Omega$, that are homologically trivial. Here $L' \in \mathbb{Z}$ is the linking number between γ and γ_1' (slightly deformed outside Ω, in order that there is no intersection with γ); similarly, $L \in \mathbb{Z}$ is the linking number between γ and γ_1 (slightly deformed inside Ω, in order that there is no intersection with γ). Therefore, if $\boldsymbol{w}$ is a vector field such that $\operatorname{curl} \boldsymbol{w} \cdot \boldsymbol{n} = 0$ on $\partial\Omega$ and $\boldsymbol{t}$ is the unit tangent vector on γ,

$$\oint_{\gamma} \boldsymbol{w} \cdot \boldsymbol{t} = L' \oint_{\gamma_1} \boldsymbol{w} \cdot \boldsymbol{t}_1 + L \oint_{\gamma_1'} \boldsymbol{w} \cdot \boldsymbol{t}_1'. \tag{2.29}$$

Applying this result to the Biot–Savart vector field $\mathrm{BS}(\boldsymbol{B})$, for which (from (2.26)),

$$\oint_{\gamma_1} \mathrm{BS}(\boldsymbol{B}) \cdot \boldsymbol{t}_1 = 0, \tag{2.30}$$

it follows that

$$\oint_{\gamma} \mathrm{BS}(\boldsymbol{B}) \cdot \boldsymbol{t} = L \oint_{\gamma_1'} \mathrm{BS}(\boldsymbol{B}) \cdot \boldsymbol{t}_1'. \tag{2.31}$$

Thus, by Stokes's theorem,

$$\oint_{\gamma} \mathrm{BS}(\boldsymbol{B}) \cdot \boldsymbol{t} = L \int_{\Sigma_1} \boldsymbol{B} \cdot \boldsymbol{n}, \tag{2.32}$$

where Σ_1 is a cutting surface of Ω with $\partial\Sigma_1 = \gamma_1'$. The value L can be interpreted as the number of loops of γ around the minor cross-section of the torus (say, the 'linking number' of the field line with the torus).

It is interesting to note that the field line helicity (the integral on the left-hand side of (2.32)) 'knows' about the linkage of the boundary curve with field lines inside the torus, by virtue of (2.25). This result is true for any magnetic field inside the torus, no matter how complex the field line topology. The value of the field line helicity, however, depends simply on the magnetic flux and a purely topological quantity depending only on the curve and the domain. Equation (2.32) is analogous to the voltage formula of a transformer (for a topological perspective on this formula, see Gross & Kotiuga 2004).

2.5.3. *Field line helicity on the boundary of a toroidal shell*

The Biot–Savart helicity is coincident with the general helicity, equation (2.21), in a toroidal shell by the same procedure as described for n-tori. The toroidal shell does, however, have some extra physical interpretations related to the cutting surfaces and field line helicities on the boundaries.

https://doi.org/10.1017/S0022377819000576 Published online by Cambridge University Press

As described in § 2.1, some care is required in order to identify the Σ_j cutting surfaces. Given suitable cutting surfaces, the helicity for a toroidal shell is

$$\Upsilon(\boldsymbol{B}) = \int_{\Omega} \boldsymbol{A}\cdot\boldsymbol{B} - \oint_{\gamma_1} \boldsymbol{A}\cdot\boldsymbol{t}_1 \int_{\Sigma_1} \boldsymbol{B}\cdot\boldsymbol{n}_1 - \oint_{\gamma_2} \boldsymbol{A}\cdot\boldsymbol{t}_2 \int_{\Sigma_2} \boldsymbol{B}\cdot\boldsymbol{n}_2, \tag{2.33}$$

where the notation is standard. The cutting surface Σ_1 is that shown in figure 2(*b*) and Σ_2 is that shown in figure 2(*c*). Therefore, we can label the fluxes as

$$\int_{\Sigma_1} \boldsymbol{B}\cdot\boldsymbol{n}_1 = \Psi_P, \quad \int_{\Sigma_2} \boldsymbol{B}\cdot\boldsymbol{n}_2 = \Psi_T, \tag{2.34a,b}$$

where Ψ_P and Ψ_T are the poloidal and toroidal fluxes respectively. If we select $\boldsymbol{A} = \mathrm{BS}(\boldsymbol{B})$, then the general helicity formula naturally reduces to the form of (2.27) due to the property in (2.26).

Considering the field line helicity in (2.32), there are now two separate boundaries for a (closed) field line to lie on. For a field line lying on the outer boundary of a toroidal shell, the interpretation is the same as that of a standard torus. That is, a field line twisting around the minor circumference of the torus L times will have a field line helicity of $L\Psi_T$. For a field line on the inner boundary, the path of the line integral can also be deformed into a union of circles around the major and minor circumferences of the toroidal hole. This time, however, due to the property in (2.26), the contribution to the integral from circles around the minor cross-section of the hole is zero. The non-zero contribution comes from the major cross-section, and if a field line on the inner boundary wraps around the major cross-section L times, its field line helicity is $L\Psi_P$.

2.6. *Mutual helicity*

Through the summation term on the right-hand side of (2.21), the domain topology enters explicitly into the helicity formula for multiply connected domains. This term is related to the mutual helicity (Laurence & Avellaneda 1993; Cantarella 2000), a quantity that measures the linkage of the magnetic field in two domains, Ω and Ω', say. Indeed, through (2.21) we can prove a representation formula for the mutual helicity which is equivalent to that obtained by Cantarella (2000) for domains Ω, $\Omega' \subset \mathbb{R}^3$ of arbitrary topology.

With its topological connection to the Gauss linking number (e.g. Moffatt 1969; Laurence & Avellaneda 1993), helicity is often written as

$$H_U(\boldsymbol{B}) = \frac{1}{4\pi} \int_{U\times U} \left(\boldsymbol{B}(\boldsymbol{x}) \times \boldsymbol{B}(\boldsymbol{y}) \cdot \frac{\boldsymbol{x}-\boldsymbol{y}}{|\boldsymbol{x}-\boldsymbol{y}|^3} \right) \mathrm{d}\boldsymbol{x}\,\mathrm{d}\boldsymbol{y}, \tag{2.35}$$

where U is a bounded open set (but not necessarily connected) and $\boldsymbol{B}$ is a magnetic field tangent to ∂U. If we consider two disjoint bounded domains M and N and we set $U = M \cup N$ and $\boldsymbol{B}_M = \boldsymbol{B}_{|M}$, $\boldsymbol{B}_N = \boldsymbol{B}_{|N}$, then it is easily checked that

$$H_{M\cup N}(\boldsymbol{B}) = H_M(\boldsymbol{B}_M) + H_N(\boldsymbol{B}_N) + 2H(\boldsymbol{B}_M, \boldsymbol{B}_N), \tag{2.36}$$

where

$$H(\boldsymbol{B}_M, \boldsymbol{B}_N) = \frac{1}{4\pi} \int_{M\times N} \left(\boldsymbol{B}_M(\boldsymbol{x}) \times \boldsymbol{B}_N(\boldsymbol{y}) \cdot \frac{\boldsymbol{x}-\boldsymbol{y}}{|\boldsymbol{x}-\boldsymbol{y}|^3} \right) \mathrm{d}\boldsymbol{x}\,\mathrm{d}\boldsymbol{y} \tag{2.37}$$

https://doi.org/10.1017/S0022377819000576 Published online by Cambridge University Press

is the mutual helicity. The self-helicities, $H_M(\boldsymbol{B}_M)$ and $H_N(\boldsymbol{B}_N)$, can be readily expressed by means of the Biot–Savart operator,

$$H_M(\boldsymbol{B}_M) = \int_M \mathrm{BS}(\boldsymbol{B}_M)\cdot\boldsymbol{B}_M, \quad H_N(\boldsymbol{B}_N) = \int_N \mathrm{BS}(\boldsymbol{B}_N)\cdot\boldsymbol{B}_N. \tag{2.38a,b}$$

Consider an open cube Q such that $\overline{M\cup N}\subset Q$. In this domain, we extend $\boldsymbol{B}$ by $\boldsymbol{0}$ in $Q\setminus\overline{M\cup N}$. We label this extension $\widehat{\boldsymbol{B}}$ and note that it is divergence-free in Q and tangent to ∂Q. Further, its helicity in Q coincides with that of $\boldsymbol{B}$ in $M\cup N$,

$$H_Q(\widehat{\boldsymbol{B}}) = H_{M\cup N}(\boldsymbol{B}). \tag{2.39}$$

Since Q is simply connected, we can use (2.21) with $g=0$ to write

$$H_Q(\widehat{\boldsymbol{B}}) = \int_Q \widehat{\boldsymbol{A}}\cdot\widehat{\boldsymbol{B}}, \tag{2.40}$$

where $\widehat{\boldsymbol{A}}$ is any vector potential of $\widehat{\boldsymbol{B}}$ in Q. Since $\widehat{\boldsymbol{B}}$ is vanishing outside $M\cup N$, it follows that

$$H_Q(\widehat{\boldsymbol{B}}) = \int_M \widehat{\boldsymbol{A}}_{|M}\cdot\widehat{\boldsymbol{B}}_M + \int_N \widehat{\boldsymbol{A}}_{|N}\cdot\widehat{\boldsymbol{B}}_N. \tag{2.41}$$

Using (2.21) in M (with genus g_M) and in N (with genus g_N), we have

$$\int_M \widehat{\boldsymbol{A}}_{|M}\cdot\widehat{\boldsymbol{B}}_M = \Upsilon_M(\boldsymbol{B}_M) + \sum_{j=1}^{g_M}\left(\oint_{\gamma_j^M}\widehat{\boldsymbol{A}}_{|M}\cdot\boldsymbol{t}_j^M\right)\left(\int_{\Sigma_j^M}\boldsymbol{B}_M\cdot\boldsymbol{n}_j^M\right) \tag{2.42}$$

and

$$\int_N \widehat{\boldsymbol{A}}_{|N}\cdot\widehat{\boldsymbol{B}}_N = \Upsilon_N(\boldsymbol{B}_N) + \sum_{l=1}^{g_N}\left(\oint_{\gamma_l^N}\widehat{\boldsymbol{A}}_{|N}\cdot\boldsymbol{t}_l^N\right)\left(\int_{\Sigma_l^N}\boldsymbol{B}_N\cdot\boldsymbol{n}_l^N\right). \tag{2.43}$$

Using (2.27), $H_M(\boldsymbol{B}_M)=\Upsilon(\boldsymbol{B}_M)$ and $H_N(\boldsymbol{B}_N)=\Upsilon(\boldsymbol{B}_N)$. Substituting these results into (2.42) and (2.43) and then substituting these into (2.36), the mutual helicity is found to be

$$\begin{aligned} H(\boldsymbol{B}_M,\boldsymbol{B}_N) \;=\; \frac{1}{2}\Bigg[&\sum_{j=1}^{g_M}\left(\oint_{\gamma_j^M}\widehat{\boldsymbol{A}}_{|M}\cdot\boldsymbol{t}_j^M\right)\left(\int_{\Sigma_j^M}\boldsymbol{B}_M\cdot\boldsymbol{n}_j^M\right)\\ &+\sum_{l=1}^{g_N}\left(\oint_{\gamma_l^N}\widehat{\boldsymbol{A}}_{|N}\cdot\boldsymbol{t}_l^N\right)\left(\int_{\Sigma_l^N}\boldsymbol{B}_N\cdot\boldsymbol{n}_l^N\right)\Bigg]. \end{aligned} \tag{2.44}$$

A careful analysis of the values of the linking numbers between γ_j^M and γ_l^N would show that this formula is equivalent to that given in Cantarella (2000). For simplicity, let us show that this is true in the case of two linked solid tori (Moffatt 1969; Laurence & Avellaneda 1993; Cantarella 2000). We have $g_M=1$ and $g_N=1$; the cycle γ_1^M is the boundary of a surface Σ_M', contained in $Q\setminus\overline{M}$, and the cycle γ_1^N is the boundary of a surface Σ_N', contained in $Q\setminus\overline{N}$. Let us also assume that the unit

https://doi.org/10.1017/S0022377819000576 Published online by Cambridge University Press

tangent vector $\boldsymbol{t}_1^M$ crosses Σ_M, the cross-section of the torus M, consistently with the direction of normal vector $\boldsymbol{n}_{\Sigma_M}$ on it, and similarly for $\boldsymbol{t}_1^N$ and the cross-section of N. In this way the linking number of M and N has value 1. By Stokes's theorem,

$$\oint_{\gamma_1^M} \widehat{\boldsymbol{A}}_{|M} \cdot \boldsymbol{t}_1^M = \int_{\Sigma'_M} \operatorname{curl} \widehat{\boldsymbol{A}} \cdot \boldsymbol{n}_{\Sigma'_M} = \int_{\Sigma'_M} \widehat{\boldsymbol{B}} \cdot \boldsymbol{n}_{\Sigma'_M}. \tag{2.45}$$

Since $\widehat{\boldsymbol{B}} = \boldsymbol{0}$ outside $M \cup N$, it follows that

$$\int_{\Sigma'_M} \widehat{\boldsymbol{B}} \cdot \boldsymbol{n}_{\Sigma'_M} = \int_{\Sigma'_M \cap N} \boldsymbol{B}_N \cdot \boldsymbol{n}_{\Sigma'_M} = \int_{\Sigma_N} \boldsymbol{B}_N \cdot \boldsymbol{n}_{\Sigma_N}. \tag{2.46}$$

Similarly,

$$\oint_{\gamma_1^N} \widehat{\boldsymbol{A}}_{|N} \cdot \boldsymbol{t}_1^N = \int_{\Sigma_M} \boldsymbol{B}_M \cdot \boldsymbol{n}_{\Sigma_M}, \tag{2.47}$$

and we obtain

$$H(\boldsymbol{B}_M, \boldsymbol{B}_N) = \left(\int_{\Sigma_M} \boldsymbol{B}_M \cdot \boldsymbol{n}_{\Sigma_M} \right) \left(\int_{\Sigma_N} \boldsymbol{B}_N \cdot \boldsymbol{n}_{\Sigma_N} \right). \tag{2.48}$$

3. Summary

In this paper we have unified the main approaches to calculating magnetic helicity in multiply connected domains. The correct approach for determining a gauge-invariant helicity is to consider the full Helmholtz decomposition, rather than the standard gauge transformation suitable for simply connected domains. We derive a gauge-invariant expression for helicity that generalizes the Bevir–Gray formula for a torus and is suitable for any connected, bounded domain in $\mathbb{R}^3$, no matter how complicated the topology.

The discovery of magnetic helicity as a topological quantity was originally made by examining Biot–Savart helicity (Moffatt 1969). We show that the general helicity formula, which holds for any vector potential, can naturally reduce to Biot–Savart helicity. The line integrals of the Biot–Savart operator on closed paths on the domain boundary can be interpreted as field line helicities, and these arise naturally from the general formula (2.21). The general form for mutual helicity is also shown to follow directly from (2.21).

In several works, a gauge-invariant helicity is found by imposing the constraint of zero flux outside the domain in question; see, for example, Chui & Moffatt (1995) for knotted domains and Taylor & Newton (2015), Hussain, Browning & Hood (2017) for periodic toroidal domains. The helicities in these works are coincident with Biot–Savart helicity by virtue of the property in (2.26).

What is clear from the general helicity formula is that the topology of the domain must be taken into account for a correct interpretation of quantities in the domain. Multiply connected domains are widely used in the context of MHD simulations. For example, a cube with two identified boundaries is equivalent to a torus topologically. Similarly, a cube with two pairs of identified boundaries is equivalent to a toroidal shell topologically. If, in such periodic domains, the magnetic field is tangent to the non-periodic boundaries, then the helicity can be interpreted in terms

https://doi.org/10.1017/S0022377819000576 Published online by Cambridge University Press

of (2.21) and, by extension, the Biot–Savart helicity (2.23). Care must be taken, however, when interpreting helicity (and other quantities) for evolving magnetic fields in periodic domains. For example, Berger (1997) discusses how periodic domains lead to strange results, such as magnetic flux ropes turning themselves inside out through magnetic reconnection. The issue here is one of mathematical modelling. That is, if a periodic domain is used to model a magnetic field in a simply connected domain, then there may be some unwanted effects due to the topology of the domain. For the (2D) flux tube example in Berger (1997, Figure 3), the behaviour shown makes perfect sense when considering the topology of the domain, the surface of a torus in this case. The behaviour, however, is physically unrealistic for a simply connected domain.

Another periodic domain that is popular in MHD simulations is the triply periodic cube. This domain, however, cannot be embedded in $\mathbb{R}^3$ and (2.21) does not apply in this case. Although it is possible to develop topological invariants in this domain (e.g. DeTurck *et al.* 2013), the physical significance of these quantities remains to investigated in depth.

REFERENCES

Alonso Rodríguez, A., Camaño, J., Rodríguez, R., Valli, A. & Venegas, P. 2018 Finite element approximation of the spectrum of the curl operator in a multiply connected domain. *Found. Comput. Math.* **18**, 1493–1533.

Arnold, V. I. & Khesin, B. A. 1992 Topological methods in hydrodynamics. *Annu. Rev. Fluid Mech.* **24**, 145–146.

Benedetti, R., Frigerio, R. & Ghiloni, R. 2012 The topology of Helmholtz domains. *Expo. Math.* **30**, 319–375.

Berger, M. A. 1984 Rigorous new limits on magnetic helicity dissipation in the solar corona. *Geophys. Astrophys. Fluid Dyn.* **30**, 79–104.

Berger, M. A. 1988 An energy formula for nonlinear force-free magnetic fields. *Astron. Astrophys.* **201**, 355–361.

Berger, M. A. & Field, G. B. 1984 The topological properties of magnetic helicity. *J. Fluid Mech.* **14**, 133–148.

Berger, M. A. 1997 Magnetic helicity in a periodic domain. *J. Geophys. Res.* **102**, 2637–2644.

Bevir, M. & Gray, J. W. 1980 Relaxation, flux consumption and quasi steady state pinches. *Proc. of RFP Theory Workshop* LA-8944-C 176–180.

Biskamp, D. 1993 *Nonlinear Magnetohydrodynamics*. Cambridge University Press.

Blank, A. A., Friedrichs, K. O. & Grad, H. 1957 Notes on magneto-hydrodynamics V. Theory of Maxwell's equations without displacement current. *AEC Research and Development Report* NYO-6486.

Cantarella, J. 2000 A general mutual helicity formula. *Proc. R. Soc. Lond.* A **456**, 2771–2779.

Cantarella, J., DeTurck, D., Gluck, H. & Teytel, M. 2000 Isoperimetric problems for the helicity of vector fields and the Biot-Savart and curl operators. *J. Math. Phys.* **41**, 5615–5641.

Cantarella, J., DeTurck, D. & Gluck, H. 2001 The Biot-Savart operator for application to knot theory, fluid dynamics and plasma physics. *J. Math. Phys.* **42**, 876–905.

Cantarella, J., DeTurck, D. & Gluck, H. 2002 Vector calculus and the topology of domains in 3-space. *Am. Math. Mon.* **105**, 409–442.

Chui, A. Y. K. & Moffatt, H. K. 1995 The energy and helicity of knotted magnetic flux tubes. *Proc. R. Soc. Lond.* A **451**, 609–629.

DeTurck, D., Gluck, H., Komendarczyk, R., Melvin, P., Shonkwiler, C. & Vela-Vick, D. S. 2013 Generalized Gauss maps and integrals for three-component links: toward higher helicities for magnetic fields and fluid flows. *J. Math. Phys.* **54**, 013515.

Dewar, R. L., Yoshida, Z., Bhattacharjee, A. & Hudson, S. R. 2015 Variational formulation of relaxed and multi-region relaxed magnetohydrodynamics. *J. Plasma Phys.* **81**, 515810604.

https://doi.org/10.1017/S0022377819000576 Published online by Cambridge University Press

EPPLE, M. 1998 Topology, matter and space 1: topological notions in 19th-century natural philosophy. *Arch. Hist. Exact Sci.* **52**, 297–392.

FARACO, D. & LINDBERG, S. 2018 Proof of Taylor's conjecture on magnetic helicity conservation. *Commun. Math. Phys.* doi:10.1007/s00220-019-03422-7.

FRANKEL, T. 2004 *The Geometry of Physics*. Cambridge University Press.

GROSS, P. W. & KOTIUGA, P. R. 2004 *Electromagnetic Theory and Computation: A Topological Approach*. Cambridge University Press.

HIPTMAIR, R., KOTIUGA, P. R & TORDEUX, S. 2012 Self-adjoint curl operators. *Ann. Mat. Pura Appl.* **191**, 431–457.

HUSSAIN, A. S., BROWNING, P. K. & HOOD, A. W. 2017 A relaxation model of coronal heating in multiple interacting flux ropes. *Astron. Astrophys.* **600**, A5.

JORDAN, R., YOSHIDA, Z. & ITO, N. 1998 Statistical mechanics of three-dimensional magnetohydrodynamics in a multiply connected domain. *Physica* D **114**, 251–272.

LAURENCE, P. & AVELLANEDA, M. 1993 A Moffatt-Arnold formula for the mutual helicity of linked flux tubes. *Geophys. Astrophys. Fluid Dyn.* **69**, 243–256.

MARSH, G. E. 1996 *Force-Free Magnetic Fields: Solutions, Topology and Applications*. World Scientific.

MOFFATT, H. K. 1969 The degree of knottedness of tangled vortex lines. *J. Fluid Mech.* **35**, 117–129.

OBERTI, C. & RICCA, R. L. 2018 Energy and helicity of magnetic torus knots and braids. *Fluid Dyn. Res.* **50**, 011413.

O'NEIL, M. & CERFON, A. J. 2018 An integral equation-based numerical solver for Taylor states in toroidal geometries. *J. Comput. Phys.* **359**, 263–282.

TAYLOR, J. B. & NEWTON, S. L. 2015 Special topics in plasma confinement. *J. Plasma Phys.* **81**, 205810501.

VALLI, A. 2019 A variational interpretation of the Biot-Savart operator and the helicity of a bounded domain. *J. Math. Phys.* **60**, 021503.

WOLTJER, L. 1958 A theorem on force-free magnetic fields. *Proc. Natl Acad. Sci. USA* **44**, 489–491.

YEATES, A. R. & HORNIG, G. 2013 Unique topological characterization of braided magnetic fields. *Phys. Plasmas* **20**, 012102.